FEATURES EXTRACTION AND CLASSIFICATION OF UTERINE MAGNETOMYOGRAPHY SIGNALS

T Ananda Babu[1], Dr. P Rajesh Kumar[2]
[1]Research Scholar, [2]Professor and Chairman, BoS
[1,2]Dept. of ECE, AUCE (A), Andhra University, Visakhapatnam, India

Abstract

The chances of morbidity and mortality of premature babies increases every year around the world. For labor prediction it is necessary to analyze the uterine physiological signals and extract the features that will change at the onset of labor. The uterine magnetomyography (MMG) presently used to measure the activity of uterine muscles. Twenty-four MMG signals from physionet database were employed for this study. Signals were divided into two groups, labor and nonlabor, depends on their days prior to delivery. The root mean square value, kurtosis and skewness coefficients, power spectrum peak frequency and median frequency, autocorrelation zero crossing, maximal Lyapunov exponent, correlation dimension, sample entropy and fractal dimension were extracted by applying different linear and nonlinear signal processing techniques. The classification of MMG signals done by evaluating the features with Naïve-Bayes, k-Nearest Neighbor (KNN) and Support Vector Machine (SVM) classifiers. KNN classifier shows better performance among the other classifiers.

Index Terms: Classification, Feature extraction, Labor, Uterine MMG

I. INTRODUCTION

The important thing in predicting labor is to analyze uterine contractions [1, 2]. At present, there are two methods that are used to record the physiological activity of the uterine: (i) the electromyography (EMG), recorded by electrodes attached to the abdomen, and (ii) the magnetomyography (MMG), based on the recording of the magnetic fields that correspond to electrical fields. The transition of the myometrium from nonlabor state to labor state can be identified by EMG/MMG. Uterine EMG/MMG parameters can indicate the myometrial properties. These properties are helpful to differentiate physiological contractions of term labor and preterm labor. Uterine MMG is a non-invasive technique and it measures the action potentials magnetic fields. The first uterine MMG activity recordings were reported in 2002 by Eswaran et al. [3]. The MMG signals have three important properties: (i) They do not depend on tissue conductivity (ii) Without making electrical contact the signals are detected outside of the body. (iii) Each sensor records only localized sources what makes them reference free.

The contraction and non-contraction segments were separated by zero crossing technique to detect the uterine contractions [4]. Uterine contractions were detected by generalized synchronization indices, assuming the electrical activity increases during the onset of delivery [5]. In [6] multiple change point estimator was used for segmentation of the MMG signal. K-means clustering algorithm (RMS and zero-crossing as candidate features) applied to these segments to detect uterine contractions. When the uterus approaches labor, the electrical activity, and its corresponding frequency increases [7]. The MMG signals were decomposed using db2 wavelet and Hilbert transform applied to each frequency band. A binary signal created by applying the clustering technique on the Hilbert amplitude. The burst contractile activity was marked by this binary decision signal [8]. The sensor space was

partitioned into four quadrants and center of gravity for each was measured for each quadrant. The delay between the pairs of quadrants (CoGs) computed by using the cross-correlation method [9]. The percentage of active sensors used to measure the propagation of MMG activity between the quadrants [10].

When the uterus approaches labor, the electrical activity, and its corresponding frequency increases. The power spectrum peak frequency of the burst activity was calculated in [11]. The contractions were analyzed using median frequency, peak frequency, kurtosis and skewness in [12]. Principal component analysis (PCA) was used to optimize the features in that study. The above studies rely on the burst activity of the signals while the RMS (root mean square) value and power spectrum median frequency were extracted from the whole 30-min signal in [13]. Non-linear signal techniques must apply to analyze uterine electrical activity, as it is a complex non-linear dynamic system. A non-linear technique, i.e. the computation of fractal dimension of the bursts yielded best results [14]. Many other non-linear techniques were employed to predict the labor [15].

The previous studies on uterine EMG/MMG were limited to the analysis of the signals for predicting labor and for the prevention of premature births. The records of term and preterm labor were separated successfully by using linear and nonlinear signal processing techniques [11, 15]. The same methodology applied to separate labor and nonlabor (antepartum) records for both term and preterm labor. In our study, the entire uterine magnetomyography signal considered to extract the following features: the signal root
mean square value, kurtosis and skewness coefficients for the signal, the signal power spectrum median frequency and peak frequency calculation, the autocorrelation zero-crossing determination, estimation of the maximal Lyapunov exponent, the correlation and fractal dimension estimation and the sample entropy calculation of the signal. All features mentioned above extracted from the complex signal (148 channels) and three individual channels that were chosen randomly. These signals were divided into two groups depends on their days to delivery after recording. Then Naïve-Bayes, k-Nearest Neighbor (KNN) and Support Vector Machine (SVM) classifiers were fed with the features for validation.

II. MATERIALS AND METHODS

A. Data Acquisition and Preprocessing

The MMG signals used in this study were downloaded from Physionet database included in the MMG database (mmgdb) [10, 21]. The database comprises uterine magnetomyography (MMG) signals recorded by using the 151 channel SQUID Array for Reproductive Assessment system (SARA) [3] installed at UAMS, Little Rock, USA. SARA is a floor-mounted passive instrument at which the mother sits and leans her abdomen on the concave surface that contains the sensor array (Fig. 1 left). The array of sensors covers 1300 cm2 surface area which is 45 cm height and 33 cm width (Fig. 1 right). The encircled sensors are MRQ2, MLL3 & MLF2 used in the present study. The entire system is in a magnetically shielded room (MSR) and is furnished with high-order synthetic gradiometer noise cancellation that eliminates the noise transmitted by the subject. The MMG signals were recorded from 25 subjects who are in the trimester of pregnancy. The signals were recorded approximately around 20 min duration. The gestation age (GA) of the subjects is in the range of 37-40 weeks and 15 subjects delivering less than 3 days after the SARA recording.

The raw signals were digitized with a sampling rate of 250 Hz. The original data was sampled at 32 Hz (down sampling). The maternal & fetal cardiac signals were attenuated by using a bandpass filter (0.1-1 Hz). The notch filter (0.25-0.35 Hz) is used to remove the maternal breathing (0.33 Hz). Segments with the maternal movement were excluded from these signals to obtain the final MMG signals. Each recording lasts around 20 min and includes 147 to 148 channels.

The original signals that were downloaded from physionet are represented in (Fig. 2). The upper trace is the complex signal comprises of total 148 sensors and the remaining are the signals of individual sensors MRQ2, MLL3 and MLF2 respectively. The sensors were chosen randomly (Fig. 1) to observe the uterine activity at different positions on pregnant abdomen.

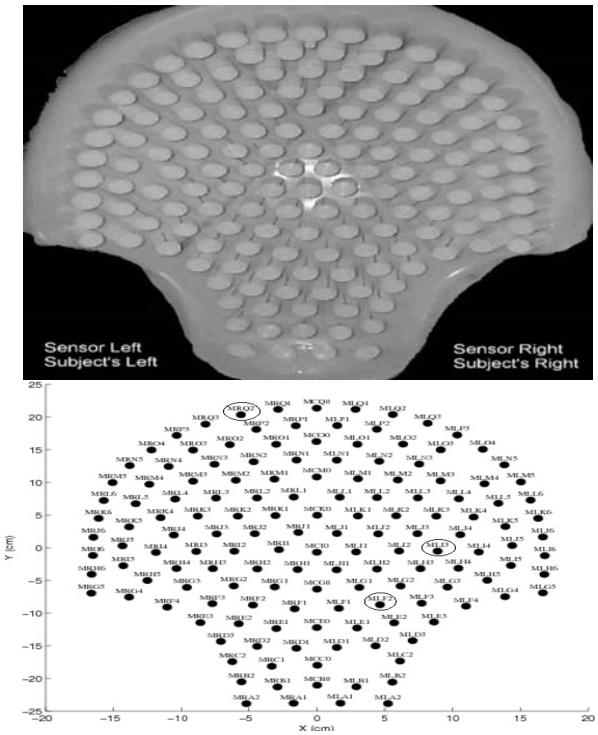

Fig.1. Front view of the arrangement of sensors (top). Sensor array with channel identification numbers (bottom).

B. Features Extraction

Feature extraction is an important part of pattern recognition. Extracted features must be effective and informative as it affects classification accuracy. The following are the features that were extracted from the multichannel signal (complex) and three individual channels (MRQ2, MLL3 and MLF2 respectively) that were chosen randomly. The extracted features should also have a meaningful electrophysiological interpretation.

Root mean square (RMS):

The root of the mean of all sample square values defined as the root mean square value of a signal which is represented in time series x (t).

$$RMS = \sqrt{\frac{1}{N}\sum_{t=1}^{N-1} x(t)^2} \quad (1)$$

where N is the length of the signal and t=0,1,…, N-1.

Kurtosis and Skewness Coefficients:

The magnitude of deviation of a probability density function from its mean defined as the skewness coefficient.

$$S = \frac{E[(x-\mu)^3]}{\sigma^3} \quad (2)$$

The tailedness of the probability density function around its mean value measured by the kurtosis.

$$K = \frac{E[(x-\mu)^4]}{\sigma^4} \quad (3)$$

where x is the random process for which μ is the mean and σ is the standard deviation. E[] is the expectation operator. The skewness and kurtosis are the third order and fourth order central moments respectively.

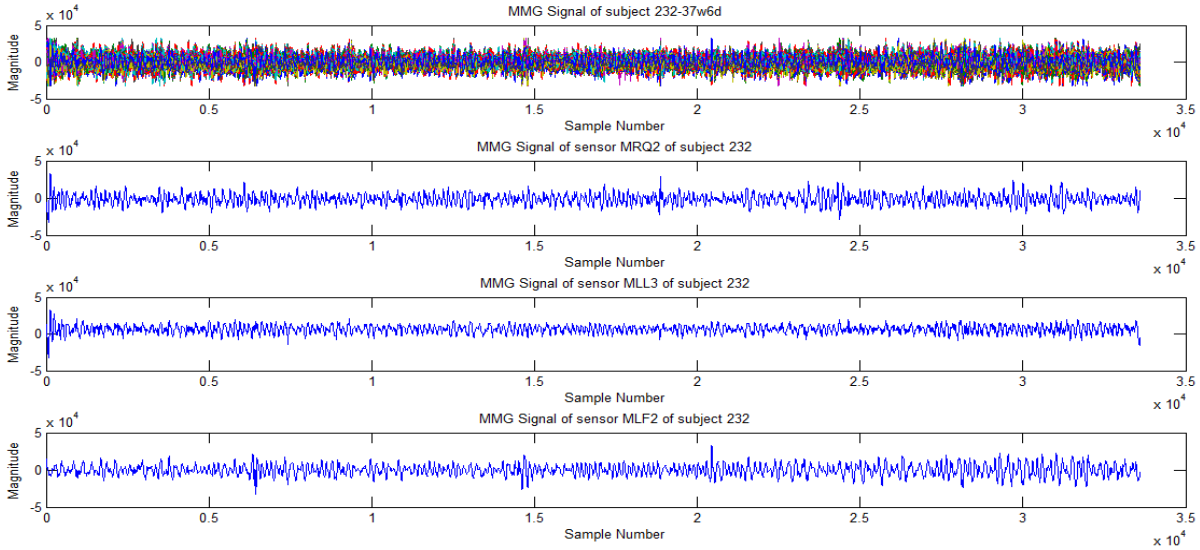

Fig. 2. MMG signals of a subject (232_37w6d) with all channels and the individual channels MRQ2, MLL3 and MLF2 respectively (from top to bottom). Subject name is in the form of ***_#GA, where *** represents the subject ID (232), and #GA refers to the gestation period in weeks and days (37w6d)

Peak frequency:

The maximum frequency of signal x(t), computed from the power spectrum (P) as:

$$f_{\max} = \arg\left(\frac{f_s}{N}\max_{i=0}^{N-1} P(i)\right) \quad (4)$$

here number of samples and sampling frequency are represented as N and fs respectively.

Median frequency:

The frequency at which the power spectrum was divided into two equal parts is the median frequency. It was calculated as:

$$f_{med} = i_m \frac{f_s}{N}, \sum_{i=0}^{i=i_m} P(i) = \sum_{i=i_m}^{i=N-1} P(i) \quad (5)$$

The power spectrum computed by using fast Fourier transform algorithm used for the calculation of frequencies.

Autocorrelation zero-crossing:

The first zero crossing after the peak of auto correlation is the auto correlation zero-crossing of the signal x(t).

$$R_{xx}(\tau_{R_{xx}}) = 0 \; R_{xx}(\tau) = \sum_{i=0}^{N-1} x(i)x(\tau + i) \quad (6)$$

here τRxx is the autocorrelation zero-crossing for the autocorrelation function Rxx.

Maximal Lyapunov exponent:

The changes in the dynamical variables of a system is demonstrated by the phase space [16]. The process of phase space reconstruction by time delayed samples is called as time-delay embedding. For a time series x(t) of length N, a Q-dimensional phase space is constructed from vectors y(t):

y(t)={yd; d=0,1,….,Q-1}

yd=(x(t+d), x(t+d+Ds),….,x(t+d+(N/Q)Ds)) (7)

where Ds is the sample delay and Q is the embedding dimension. The maximal Lyapunov exponent determines the predictability of a dynamic system (chaos). It measures the velocity of the trajectory that converges from a given point.

$$\lambda = \lim_{t\to\infty}\lim_{\|\Delta y_t\|\to 0}\frac{1}{t}\log\frac{\|\Delta y_t\|}{\|\Delta y_0\|} \quad (8)$$

where $\|\Delta y_0\|$ and $\|\Delta y_t\|$ are the Euclidean distance between two states of the system at time t_0 and time t respectively.

Correlation dimension:

The correlation dimension measures the complexity of a given time-series. It is proportional to the probability of the distance between two points on a trajectory being less than r,

$$D_{corr} = \lim_{r\to 0}\frac{\log(C(r))}{\log(r)} \quad (9)$$

where

$$C(r) = \lim_{m\to\infty}\frac{1}{M^2}\sum_{i=1}^{M}\sum_{j=i+1}^{M}\Theta(r - |y(i) - y(j)|) \quad (10)$$

and

$$\Theta(r - |y(i) - y(j)|) = \begin{cases} 1 : (r - |y(i) - y(j)|) \geq 0 \\ 0 : (r - |y(i) - y(j)|) < 0 \end{cases} \quad (11)$$

To calculate λmax and Dcorr, we used a practical method described in [7].

Sample entropy:

The sample entropy measures the regularity of finite length time series. From a time series x(t) of length N, patterns aj(0,…,n-1) of length n (n<N) were defined as aj(i) = x(i + j) where i=0,1,…,n-1 and j=0,1,…,N-n. If |x(ts + i)-aj(i)| ≤ r for each 0 ≤ i < n then x(ts,…,ts+n-1) is considered as a match for a pattern aj. The number of pattern matches cn constructed for each n. Then the sample entropy defined in the equation (12).

$$SampEn_{n,r}(x) = \begin{cases} -\log(c_n / c_{n-1}) : c_n \neq 0 \wedge c_{n-1} \neq 0 \\ -\log((N-n)/(N-n-1)) : c_n = 0 \vee c_{n-1} = 0 \end{cases} \quad (12)$$

The parameter r varied from 1.0 to 2.0 in steps of 0.125 and the parameter n taken as either 2 or 3 or 4 for the evaluation purpose.

Fractal Dimension:

Fractal dimension measures the complexity of time domain signal [17]. A self-similar time series X_k^n calculated from original sequence x(t) as: X_k^n = x(n), x(n+k), x(n+2k),……,x(n+int[(N-n)/k]k) (13)

here n and k are initial time and time interval respectively where int[] represents the integer part of. The length of the curve Ln(k) was computed for each of the k time series as:

$$L_n(k) = \frac{1}{k}\left[\left(\sum_{i=1}^{\mathrm{int}\left[\frac{(N-n)}{k}\right]}|x(n+ik) - x(n+(i-1)k)|\right)\frac{N-1}{\mathrm{int}\left[\frac{N-n}{k}\right]k}\right] \quad (14)$$

Where N is the length of X and (N-1)/{int[(N-n)/k]k} is a normalization factor. Ln(k) was averaged for all n forming the mean value of the curve length L(k) for each k = 1,…, kmax as

$$L(k) = \frac{\sum_{n=1}^{k} L_n(k)}{k} \quad (15)$$

From the equation (15) an array of mean values L(k) was obtained. Then the HFD was estimated as the slope of least squares linear best fit from the plot of ln(L(k)) versus ln(1/k):

$$HFD = \frac{\ln(L(k))}{\ln(1/k)} \quad (16)$$

C. Classification

The feature values were divided into two groups depends on the subject's days to delivery after recording. One group has the records of subjects that delivered within 48 hours after recording (Labor) while the other group delivered after 48 hours (Antepartum). The Naïve-Bayes is a simple classification algorithm that can be applied to physiological signals [18]. It has many applications like spam mail filtering, medical diagnosis and weather forecasting. It estimates the class probability, by using Bayes theorem assuming that the features of one class is independent from the other. The classifier works well, even though the conditional independence assumption does not hold. Naïve-Bayes algorithm has received a great attention because of its simplicity and effectiveness in implementation as well as it is highly practical in day to day problems. An advantage of the naive Bayes classifier is that it only requires a small amount of training data to estimate the parameters (means and variances of the variables) necessary for classification.

K nearest neighbor (KNN) classifier can be used in many applications like speech recognition, astronomical object classification, for predicting heart attacks and for classification of uterine contractions during labor [19]. The data samples will be classified depends on their nearest neighbor class. K nearest neighbor is one of the widely used data mining technique in classification. Data with labels is used to train the classifier. Then for a given test data, whose label is not known, and which is presented by a vector in the feature space, calculate the distances between it and every point in the training data set. After sorting distances, the decision of the class label of the test point is made according to the label of the k nearest points in the training data set. KNN classifier is also known as memory based classification. KNN classifier based on hamming distance metric used in our research.

Support vector machine (SVM) is a powerful classification technique that can be applied to uterine physiological signals [20]. Primarily, it was implemented for two-class classification problems. Multiple classes can be classified by combining multiple binary SVMs. The optimization criterion is the width of the margin between the classes, i.e., the empty area around the decision boundary (the separating hyperplane) defined by the distance to the nearest training patterns. These patterns, called support vectors, finally define the classification function. Linear kernel, sigmoid kernel, polynomial kernel, and RBF kernel are most commonly used kernel functions. In our work, we used Gaussian Radial Basis Function (RBF) kernel. Supervised algorithms are sensitive to the division of feature dataset into training feature and testing feature sets. In this work we divided the dataset into three parts. The classifiers were trained with 2/3 of dataset while the remaining used as the test dataset.

III. RESULTS AND DISCUSSION

Confusion matrix is a two-dimensional table with a row and a column for each class. Each element of the matrix shows the number of test examples for which the actual class is the row and the predicted class is the column. The confusion matrices showing the classification results of the Naïve-Bayes, KNN and SVM classifiers for different signals are given in Table1.

The classifiers were evaluated using accuracy as the performance metric and computed as follows:

$$Accuracy = \frac{(TP + TN)}{(TP + TN + FP + FN)} \quad (17)$$

where TP, TN, FP and FN represents the true positives, true negatives, false positives and false negatives obtained after the classification. The overall accuracy values for different classifiers are shown in table 2.

According to the confusion matrices for Naïve-Bayes classifier, 3 nonlabor (antepartum) subjects were classified incorrectly for the multichannel and MLF2 channel while these subjects were correctly classified for the other channels. In fact, for those channels the labor subjects (2) were misclassified by this classifier. The labor subjects were classified efficiently by the KNN classifier for all the signals but it misclassifies the nonlabor subjects (either 1 or 2) as shown in the table 1. The SVM classifier

classifies the labor subjects correctly for all the signals except MLL3 sensor where 3 subjects were misclassified as nonlabor subjects. This classifier was unable to classify the nonlabor subjects, for MRQ2 sensor no nonlabor subjects were present.

Table 1. Confusion Matrices for Naïve-Bayes, KNN and SVM Classifiers of Complex Signal, MRQ2, MLL3 and MLF2 Channels respectively.

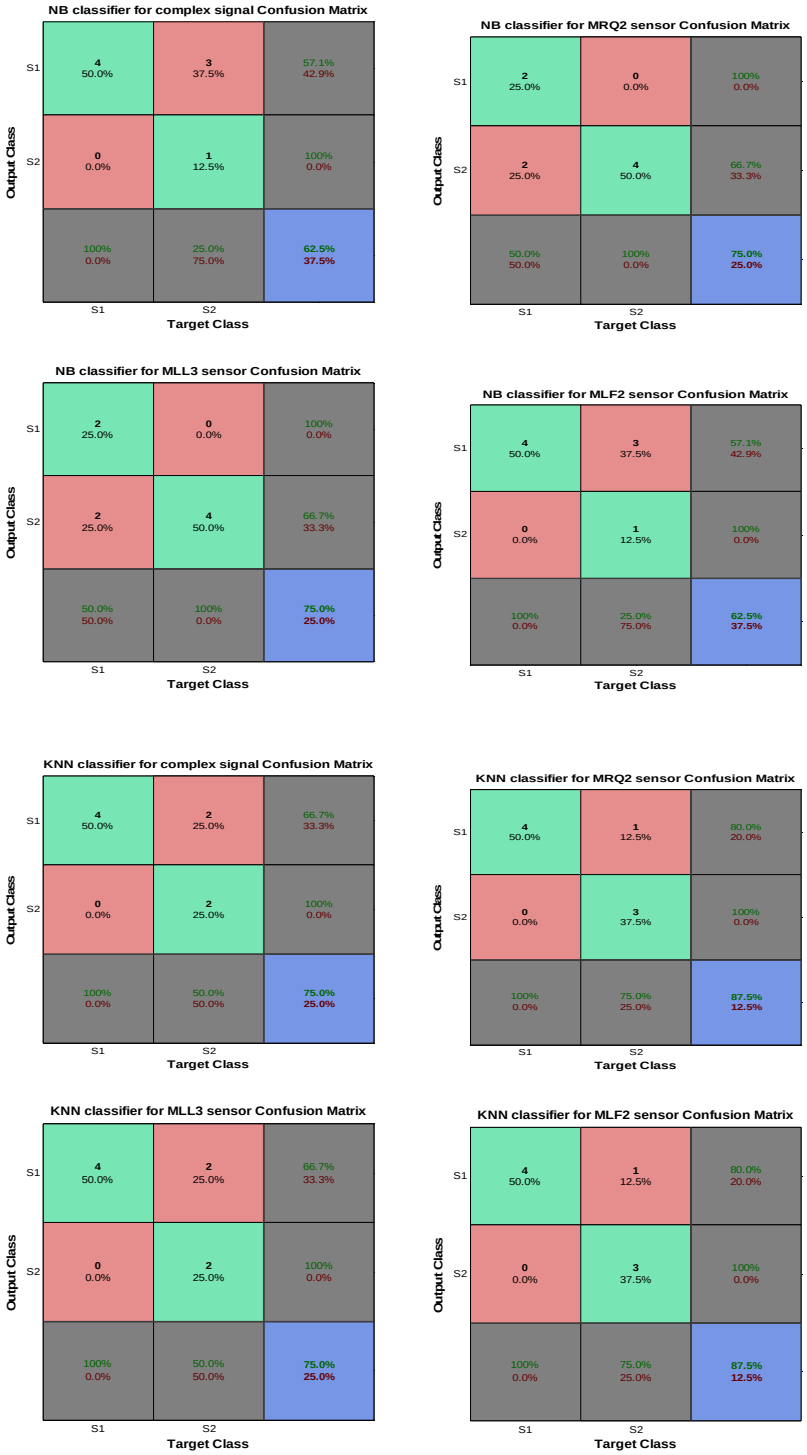

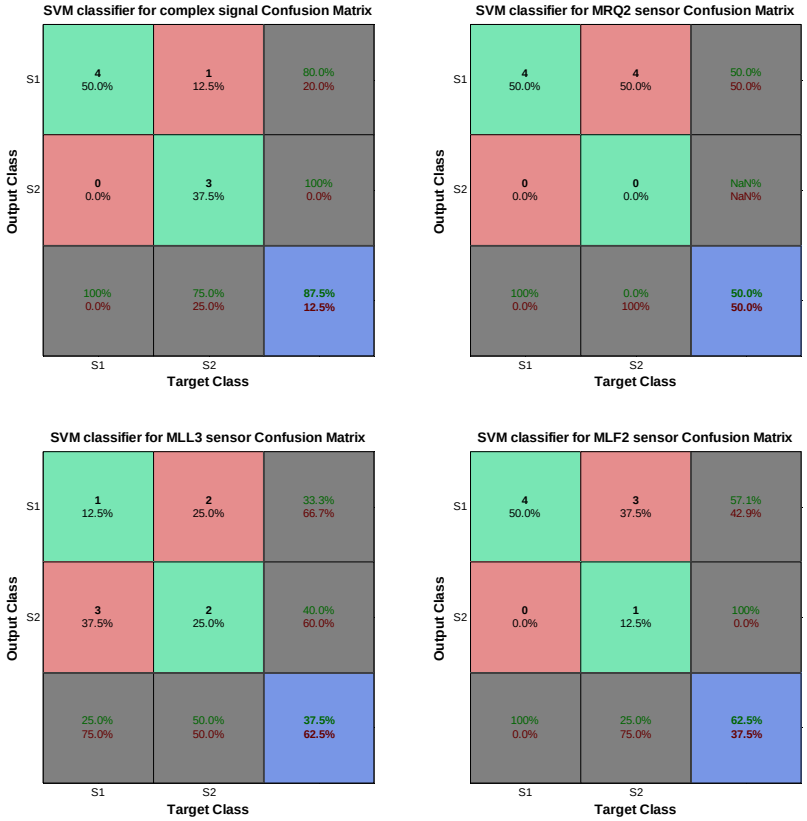

The performance of the classifiers were compared by using the classification accuracy as the performance metric (Table 2). The misclassification of even a single subject leads to drastic changes in accuracy which is reflected in the table2. The Naïve-Bayes classifier accuracy for the multichannel and MLF2 channel (62.5%) are less than that of MRQ2 and MLL3 channel (75%). The KNN classifier had a better classification accuracy (87.5% for MRQ2 and MLF2 sensor and 75% for both multichannel and MLL3 channel) compared with the other classifiers. The SVM classifier shows very low accuracy (37.5% and 50%) though the accuracy of complex (87.5%) and MLF2 sensor (62.5 %) were comparable with the remaining classifiers.

Table 2. The Classification Accuracy Values of Naïve-Bayes, KNN and SVM Classifiers for Different Signals.

	Naïve-Bayes (%)	KNN (%)	SVM (%)
Complex	62.5	75	87.5
MRQ2	75	87.5	50
MLL3	75	75	37.5
MLF2	62.5	87.5	62.5

The MMG signals used in the study were divided into two groups based on the fact that the electrical activity of the myometrium increased at the onset of labor. The maternal factors that could affect the onset of labor were not considered for our study. The maternal factors like Gestation Age (GA), Body Mass Index (BMI) and cervical dilation/effacement may be similar to the subjects that delivered within one day and two days. These subjects were in two different groups which imposes a limitation to our study. This adversely affects the classifier's accuracy which is clear in case of Naïve-Bayes classifier. Naïve-Bayes works on the assumption that all features are conditionally independent given the class label. Though the assumption violated in our study, still it gives reasonable accuracy.

The ultimate goal of feature extraction is to provide the parameters that would distinguish the records between labor and nonlabor subjects effectively. But the sample entropy gave non-numeric values for some subjects. SVM classifier accuracy is greatly influenced since the rows with those non-numeric values were ignored during classification. The attempt to make use of other kernels (linear and polynomial) did not yield good results. Our aim

is not the position of sensor which has high contractile burst activity so the sensors were chosen randomly. Since each sensor provides only localized information, our research limited to compare the performance of classifiers for a particular sensor. The methods employed are not useful for hospital work as the cost of the SARA system is very high. But from a research point of view, it gives a great opportunity to get the knowledge about the physiology of parturition.

IV. CONCLUSION

A lot of research is going on for the prediction of labor by analyzing the uterine MMG signals. The entire signal considered for this study without separating contraction and non-contraction periods. The RMS value, kurtosis, skewness coefficient, power spectrum median and peak frequencies, autocorrelation zero-crossing, maximal Lyapunov exponent, correlation and fractal dimensions and sample entropy were extracted by applying linear and nonlinear signal processing techniques. The subjects were divided into two groups depends on their time prior to delivery. The KNN classifier efficiently classified the signals with better classification accuracy than Naïve-Bayes and SVM classifiers.

Though the present work carried out on term records, it can be applied to preterm records for the prediction of preterm birth. The present study limited to only 24 subjects, so in the future these methods will be applied to the larger population of data. If the physicians are able to differentiate the true and false labor, then the unwanted hospital visits and treatments will be reduced. Prediction of premature labor will curb the morbidity and mortality of new born babies.

REFERENCES

[1] J. Gondry, J. Duchene, and C. Marque, "First results on uterine EMG monitoring during pregnancy," Proc. Ann. Int. Conf. IEEE EMBS, 1992, vol. 6,, pp. 2609-2610.

[2] Eswaran H, Preissl H, Wilson JD, Murphy P, Lowery CL. "Prediction of labor in term and preterm pregnancies using non-invasive magnetomyographic recordings of uterine contractions," Am J of Obstet Gynecol. 2004; 190[6]:1598–1603.

[3] Eswaran H, Preissl H, Wilson JD, Murphy P, Robinson SE, Lowery CL. "First magnetomyographic recordings of uterine activity with spatial-temporal information with a 151-channel sensor array," Am. J. Obstetrics Gynecology 2002;187:145–51.

[4] Radhakrishnan N, Wilson JD, Lowery C, Eswaran H, Murphy P. "A fast algorithm for detecting contractions in uterine electromyography," IEEE Eng. Med. Biol. Mag 2000;19:89–94. [PubMed: 10738666].

[5] Ramon C, Preissl H, Murphy P, Wilson JD, Lowery CL, Eswaran H. "Synchronization analysis of the uterine magnetic activity during contractions," Biomed. Eng. Online 2005;4:55. [PubMed: 16197557].

[6] La Rosa PS, Nehorai A, Eswaran H, Lowery CL, Preissl H. "Detection of uterine MMG contractions using a multiple change point estimator and the k-means cluster algorithm," IEEE Trans. Biomed. Eng 2008;55:453–67. [PubMed: 18269980].

[7] Garfield RE, Maner WL, MacKay LB, Schlembach D, Saade GR. "Comparing uterine electromyography activity of antepartum patients versus term labor patients," Am. J. Obstetrics Gynecology 2005;193:23– 9.

[8] Furdea A, Eswaran H, Wilson JD, Preissl H, Lowery CL, Govindan RB. "Magnetomyographic recording and identification of uterine contractions using Hilbert-wavelet transforms," Physiological measurement. 2009;30[10]:1051-1060. doi:10.1088/0967-3334/30/10/006.

[9] Furdea A, Preissl H, Lowery CL, Eswaran H, Govindan RB. "Conduction velocity of the uterine contraction in serial magnetomyogram (MMG) data: Event based simulation and validation" In 2011 Conf Proc IEEE Eng Med Biol Soc. 2011;6025–6028. doi: 10.1109/IEMBS.2011.6091489 [PubMed: 22255713].

[10] Escalona-Vargas D, Govindan RB, Furdea A, Murphy P, Lowery CL, Eswaran H. "Characterizing the Propagation of Uterine Electrophysiological Signals Recorded with a MultiSensor Abdominal Array in Term Pregnancies," PLoS ONE [2015] 10[10]: e0140894. doi:10.1371/journal. pone.0140894.

[11] Garfield RE, Maner WL, MacKay LB, Schlembach D, Saade GR. "Comparing

uterine electromyography activity of antepartum patients versus term labor patients," Am. J. Obstetrics Gynecology 193:23–9 (2005).

[12]Leman H, Marque C, Gondry J, "Use of the electrohysterogram signal for characterization of contractions during pregnancy," IEEE Transactions on Biomedical Engineering 46(10):1222–1229 (1999).

[13]Verdenik I, Pajntar M, Leskosek B "Uterine electrical activity as predictor of preterm birth in women with preterm contractions," Eur J Obstet Gynecol Reprod Biol 95(2):149–153 (2001).

[14]Maner WL, MacKay LB, Saade GR, Garfield RE "Characterization of abdominally acquired uterine electrical signals in humans, using a non-linear analytic method," Med Biol Eng Comput 44(1–2):117–123 (2006).

[15]Fele-Zorz, G. Kavsek, Z. Novak Antolic and F. Jager "A comparision of various linear and non-linear signal processing techinques to separate uterine EMG records of term and pre-term delivery groups," Med. Biol. Eng. Comput 46:911-922 (2008).

[16]Nagarajan P, Eswaran H, Wilson J, Murphy P, Lowery C, Preisl H "Analysis of uterine contractions: a dynamical approach," Jrnl. of Matern Fetal Neonatal Med 14:8–20 (2003).

[17]Srdjan Kesic, Sladjana Z. Spasic "Application of Higuchi's fractal dimension from basic to clinical neurophysiology: A review," Elsevier, Computer methods and programs in biomedicine 133:55–70 (2016).

[18]Juliano Machado, Alexandre Balbinot , "Executed movement using EEG signals through a Naïve-Bayes classifier," Micromachines 2014, 5, 1082-1105; doi:10.3390/mi5041082.

[19]R jyothi, S Hiwale and PV Bhat, "Clssification of labour contractions using KNN classifier," Proc. Of 2016 Int. Conf. on systems in medicine and biology, 2016.

[20]Moslem B, Khalil M, Diab MO, Marque C,"Combining multiple support vector machines for boosting the classification accuracy of uterine EMG signals," 2011 18th IEEE Intl. Conf. on Electronics, Circuits, and Systems, Beirut, Lebanon: doi:10.1109/ICECS.2011.6122354.

[21]Goldberger AL, Amaral LAN, Glass L, Hausdorff JM, Ivanov PCh, Mark RG, Mietus JE, Moody GB, Peng C-K, Stanley HE. PhysioBank, PhysioToolkit, and PhysioNet: Components of a New Research Resource for Complex Physiologic Signals. Circulation 101(23):e215-e220 [Circulation Electronic Pages; http://circ.ahajournals.org/cgi/content/full/101/23/e215]; 2000 (June 13).